

Small Scale Stability of Isolated Rural Microgrid Based on Load Characteristics

Vinit Kumar Singh, Ashu Verma, T. S. Bhatti



Abstract: Rural areas are either weakly connected to grid or have no grid access. Therefore, hybrid system is only solution for continuous uninterrupted power supply. Also these rural microgrids have specific types of load. Small systems are more vulnerable to load disturbances and therefore, frequency and voltage variation have post disturbance effect on the system stability. Four different types of loads having exponential voltage and frequency characteristics are considered for the study. EPRI Load modeling has been considered based on aggregate index calculation. The system is studied for step increase/decrease in load as well as input power to the wind energy system and also the post effect of voltage & frequency change on the load with its influence on the system is considered for study purpose. The isolated microgrid proposed has wind energy system with PMSG and biogas genset (BG) with synchronous generator (SG). The system is designed in such a way that any increase/decrease in load and input power to wind is taken up by the biogas system. No additional reactive power compensator is envisaged. Accordingly, the controllers are tuned using Integral Square Error criterion for mitigate variation in load voltage & frequency.

Keywords: Microgrid, renewable energy, wind energy system(WES), biogas generator(BG), synchronous generator, permanent magnet synchronous generator.

I. INTRODUCTION

Rural microgrids are small power system installed in distant topographical areas either isolated from the system grid or with an erratic grid connection [1]. In isolated system conventionally diesel generators (DG) was the main source however, when combined with renewable energy sources have developed into hybrid system. But with modification in the engine, biogas can be used as alternate fuel to diesel. Compression Ignition (CI) engine with diesel as pilot fuel can use biogas for running the engine [2]. Wind, Solar and Hydro are three major cradles of renewable energy. These renewable energy are site dependent, proper wind speed is

needed for wind power, solar irradiation for PV system and a hydro stream is needed for hydro power. The main interest in combining BG with renewable is vested on low cost and uninterrupted supply. Many papers have been published in which different type of generators are combined with renewable sources and carried out analysis with dynamic studies. Induction generator (IG) is one of the electromechanical conversion device used with sources intermittent in nature like wind energy system (WES). IG therefore, has proven good replacement against the synchronous generator [3]. However, Induction generator requires reactive power therefore; excitation capacitor is used in case of Self excited induction generator (SEIG). Various effort has been made by researchers to tackle the problem [4][5]. Wind with PMIG, DG with SG and Statcom has been proposed for meeting the reactive power requirements [6]. The other alternative is Permanent magnet synchronous generator (PMSG). The PMSG has attracted more and more attention due to its advantages of high efficiency and reliability [7]. Compared with IG, PMSG have the following benefits: (a) PMSG allows the generator to function at less speed without a gearbox i.e. directly driven. This lessens the dimensions and weightiness of nacelle equipment, mechanical losses associated with gear system in operation as well as operation & maintenance necessities. (b) PMSG supports the grid voltage by generating more reactive power as it is interfaced with the power system through converter which has coupling capacitor. These assets have made PMSG become prevalent, even though there are converter losses [8][9]. Generally in biogas sets synchronous generator (SG) are used. SG is accompanied with excitation system which has automatic voltage regulator [10]. The frequency and power output can be controlled by the speed governor and actuator of the biogas engine. The gas engine model with electronic governor and induction generator was used as a biogas generator [11]. The dynamic stability analysis was conducted in that study and the system was found to be stable with all the Eigen values lying on the left-hand side of the complex s plane. Various other models for stability analysis and control schemes for biogas have been studied by the researchers [12][13]. The active power control action of a biogas engine is quite slow as compared to the inverter controlled distributed generation sources. When there is disturbance in the system different type of load shows different characteristics. Loads are basically dependent on frequency, voltage and recovery time [14].

Manuscript received on May 25, 2020.
Revised Manuscript received on June 29, 2020.
Manuscript published on July 30, 2020.

* Correspondence Author

Vinit Kumar Singh*, Centre of Eney Studies, Indian Institute of Technology, New Delhi, India. Email: singhvinitk@gmail.com

Dr. Ashu Verma, Centre of Eney Studies, Indian Institute of Technology, New Delhi, India. Email: Ashu.Verma@ces.iitd.ac.in

Dr. T.S. Bhatti, Centre of Eney Studies, Indian Institute of Technology, New Delhi, India. Email: T.S.Bhatti@ces.iitd.ac.in

© The Authors. Published by Blue Eyes Intelligence Engineering and Sciences Publication (BEIESP). This is an open access article under the CC BY-NC-ND license (<http://creativecommons.org/licenses/by-nc-nd/4.0/>)

Small Scale Stability of Isolated Rural Microgrid Based on Load Characteristics

Various types of load modeling have been proposed in literature considering static and dynamic characteristics of load based on component level approach and measurement based approach [15]. EPRI load modeling based on voltage change and frequency change is one of the solutions for composite type of load as it gives more realistic results [16]. Various papers are written analyzing control strategy for frequency and voltage control of wind-biogas/diesel based hybrid system [10][17]. The other discuss about the economics involved with the feasibility of the system [18]. However, very less attention has been paid on the isolated small system considering post disturbance effect of load on the system stability.

Present work is motivated by dynamic stability study of small isolated system with EPRI load modeling considering the post effect of load on the system due to frequency and voltage variation. The paper is ordered as follows:

Section-II gives the detail of the system considered for investigation. Section-III comprises of description regarding modeling of isolated microgrid and its associated load. Section-IV discuss about the simulation of the system and results. Finally, section-V is the conclusion of the paper under consideration.

II. SYSTEM CONSIDERED FOR INVESTIGATION

The system modeling consist of isolated rural microgrid of 500 kW rating comprising of 250 kW BG and 250 kW WES system as shown in Fig.1 and the system data details are given in Table I of Appendix. The objective of the study is variation in the state variables of the isolated small system due to load variations and variation in input power to the renewable energy source. The load variation is characterized by deviation in voltage and frequency of the system. Small systems are more liable to disturbances, therefore, the controller needs to act very fast to minimize the error and reach steady state. Further bifurcation of load into segments helps to establish the effect of voltage and frequency variation on the system. The rural microgrid system generally comprises of specific type of load like residence load, agriculture pump, lighting etc. In the paper four types of load is considered for modeling as indicated in Table IV of Appendix. Whenever the load increases the system voltage and frequency decreases and when the load decreases the same increases. The load modeling is done combining exponential model with frequency based load model. Aggregate indices of the individual components of load in exponential model and frequency based load model are calculated based on proportion (rated kW of particular load/total kW) of various load types in the system. As the system is small therefore, to establish the voltage stability, reactive power compensation is provided by the excitation system associated with the BG. No additional reactive power compensation equipment is envisaged. The novel approach is proposed in rural microgrid considering component based load modeling based on frequency and voltage deviation and its post effect on system stability along with control strategy to mitigate the frequency and voltage oscillation within limits.

III. MODELING OF SYSTEM

The line diagram of the scheme considered is shown in Fig.1. Any change in demand or generation results in imbalance in power flow which is compensated by increase or decrease in active power and reactive power generation through the generator. The system power balance Equations are given by

$$P_{bg} + P_w = P_l \quad (1)$$

$$Q_{bg} + Q_w = Q_l \quad (2)$$

Small disturbance in the power can be represented by

$$\Delta P_{bg} + \Delta P_w = \Delta P_l \quad (3)$$

$$\Delta Q_{bg} + \Delta Q_w = \Delta Q_l \quad (4)$$

Deviation of active and reactive power generation due to load variation will result in frequency and voltage to change, which can be expressed by Equation based on state space using Laplace transform as

$$\Delta F(s) = \frac{K_{ps}}{1+sT_{ps}} [\Delta P_{bg}(s) + \Delta P_w(s) - \Delta P_l(s)] \quad (5)$$

$$\Delta V(s) = \frac{K_{vs}}{1+sT_{vs}} [\Delta Q_{bg}(s) + \Delta Q_w(s) - \Delta Q_l(s)] \quad (6)$$

Where, K_{ps} , K_{vs} , T_{ps} and T_{vs} are the system gain and time constant. P_w , P_{bg} and P_l are active Power of wind energy system, biogas genset and load respectively. Q_w , Q_{bg} and Q_l are reactive Power of wind energy system, biogas genset and load respectively.

The calculated value of different parameters is given at Appendix.

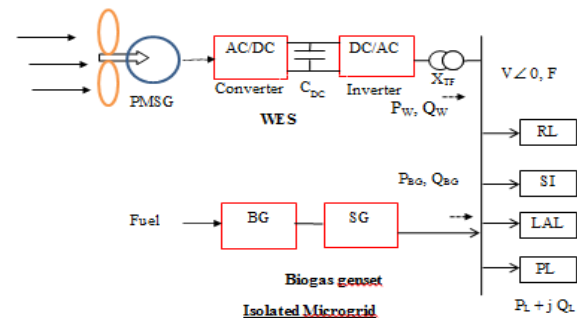


Fig.1, Line diagram of proposed isolated rural microgrid.

A. Modeling of Inverter connected to WES.

The WES comprises wind turbine, generator & auxiliaries coupled with Buck Boost Converter. The power output from WES depends upon the wind speed therefore, keeps on changing as per speed of wind. However, the controllers attached are tuned to extract required power from the turbine to be fed to the generator to maintain constant power output. Also the controllers of the inverter are tuned to compensate small perturbation in the power requirement of the system. WES side converter transmits the power to the load end inverter through a coupling capacitor between converters. The coupling capacitor helps in maintaining constant voltage across it.

The DC to AC converter produces power corresponding to the requirement of the system. In addition, the WES inverter also maintains the system reactive power balance. A small signal model of the WES inverter is developed using active and reactive power flow equations from the Inverter model. The Equations are as

$$P_w = \frac{V_{inv}V\sin(\delta_{inv})}{X_{TW}} \tag{7}$$

$$Q_w = \frac{V_{inv}V\cos(\delta_{inv})-V}{X_{TW}} \tag{8}$$

For small incremental change in power flow of the Inverter, (7) and (8) can be written as

$$\Delta P_w(s) = K_1\Delta\delta_{inv}(s) + K_2\Delta V_{inv}(s) + K_3\Delta V(s) \tag{9}$$

$$\Delta Q_w(s) = K_4\Delta\delta_{inv}(s) + K_5\Delta V_{inv}(s) + K_6\Delta V(s) \tag{10}$$

The parameters/constants $V_{inv}\Delta\delta_{inv}$ and X_{TW} are input inverter voltage and reactance of coupling transformer. K_1, K_2, \dots, K_6 are constant of the above mentioned equations associated with state variables. The values of parameter are given in Table III of Appendix.

The transfer function of the PVS considering Inverter side active and reactive power control is shown in Fig. 2.

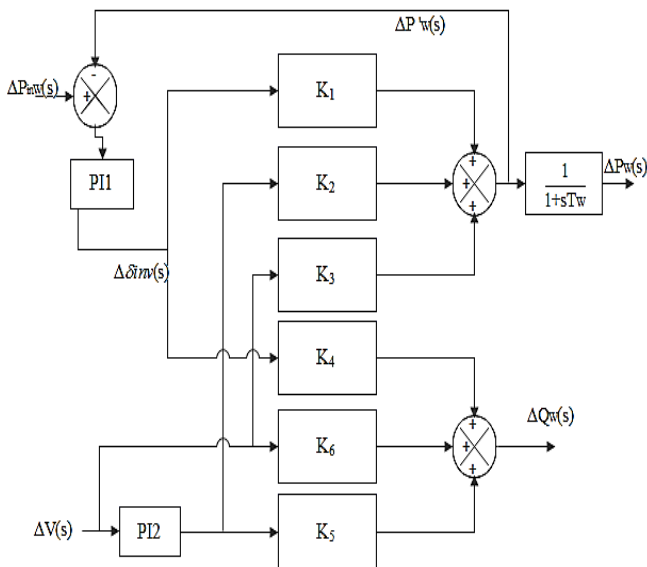


Fig. 2, Transfer function model of PV Inverter.

B. Modeling of Biogas Generator set

A biogas engine is connected to a synchronous generator, which generates electricity. The reactive power generation and voltage is controlled by the AVR and real power generation is controlled by speed governor control mechanism.

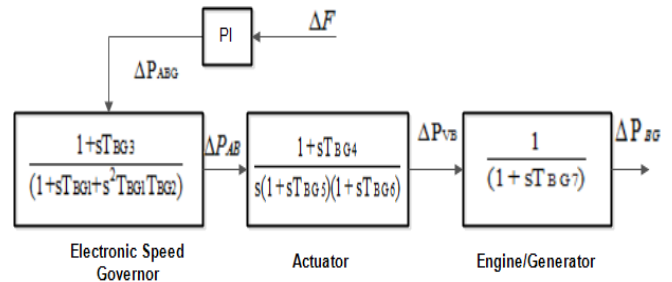


Fig.3, Transfer function model of biogas-genset for active power control.

The block diagram of biogas system having electronic speed governor is shown in Fig. 3. TBG1 to TBG7 are time constant of Biogas Engine mechanism.

The regulatory valve supplies biogas to the engine. Valve position is regulated by the actuator which depends on signal from the speed governor. The signal is generated in response to frequency and voltage angle change. The change in active power output of the biogas-genset is given by

$$\Delta P_{BG}(s) = \frac{1}{1 + sT_{BG7}} \Delta X_{VB}(s) \tag{11}$$

$$\Delta X_{VB}(s) = \frac{(1 + sT_{BG4})}{s(1 + sT_{BG5})(1 + sT_{BG6})} \Delta X_{ABG}(s) \tag{12}$$

The adjustment in the actuator input signal depends upon the speed governor design and it is given by

$$\Delta X_{AB}(s) = \frac{(1 + sT_{BG3})}{(1 + sT_{BG1} + s^2T_{BG1}T_{BG2})} \Delta P_{CB}(s) \tag{13}$$

An IEEE type-I excitation control with saturation neglected as shown in Fig. 4 is considered. The small deviance in voltage behind transient reactance, $\Delta E'_{qB}$, is given by

$$(1 + sT_{GB})\Delta E'_{qB} = [K_{1BG} \Delta E_{fdB}(s) + K_{2BG}K\Delta V(s)] \tag{14}$$

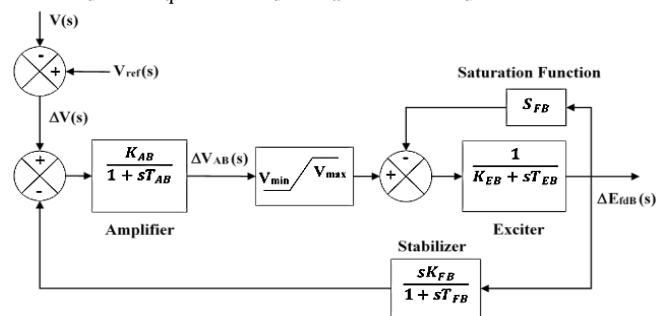


Fig.4, Model of excitation control system for biogas-genset (IEEE Type-I).

For small deviance in voltage, the reactive power delivered by the biogas-genset is given by

$$\Delta Q_B(s) = [K_{3BG}\Delta E'_{qB}(s) + K_{4BG}\Delta V(s)] \tag{15}$$

Assuming that SG is operates at constant pf, the reactive power variation due to change in active power is given by

$$\Delta Q'_{BG}(s) = K_{rb} \Delta P_{BG}(s) \tag{16}$$

C. System Load Modeling

The active power and reactive power equations for EPRI load model is given below. This model is used for dynamic studies and gives good results for the small system.

$$P_l = P_0 [P_{C1} (\frac{V}{V_0})^{K_{np1}} \{1 + N_{npf}(f - f_0)\} + (1 - P_{C1}) (\frac{V}{V_0})^{K_{np2}}] \tag{17}$$

$$Q_l = P_0 \left[Q_{C1} \left(\frac{V}{V_0}\right)^{K_{nq1}} \{1 + N_{nqf1}(f - f_0)\} + \left(\frac{Q_0}{P_0} - Q_{C1}\right) \left(\frac{V}{V_0}\right)^{K_{nq2}} \{1 + N_{nqf2}(f - f_0)\} \right] \tag{18}$$

P_0 , Q_0 , V_0 and f_0 are active power, reactive power, the bus voltage and the frequency, prior to the disturbance. P_{C1} is frequency dependent fraction of real load, Q_{C1} is the reactive load coefficient of uncompensated reactive load to real power load, K_{np1} and K_{np2} are the voltage exponents for frequency dependent and frequency independent active power load, K_{nq1} and K_{nq2} are voltage exponents for uncompensated and compensated reactive power load, N_{npf} and N_{nqf1} are the frequency sensitivity coefficients for real and uncompensated reactive power load and N_{nqf2} is frequency sensitivity coefficient for compensated reactive power load. The incremental decrease in load results in increase in voltage by ΔV and frequency by Δf . Equations (17) & (18) can be rewritten as

$$P_l = P_0 \left[[P_{C1} \left(\frac{V_0 + \Delta V}{V_0}\right)^{K_{np1}} \{1 + N_{npf}(\Delta f)\} + (1 - P_{C1}) \left(\frac{V_0 + \Delta V}{V_0}\right)^{K_{np2}}] \right] \tag{19}$$

$$Q_l = P_0 \left[Q_{C1} \left(\frac{V_0 + \Delta V}{V_0}\right)^{K_{nq1}} \{1 + N_{nqf1}(\Delta f)\} + \left(\frac{Q_0}{P_0} - Q_{C1}\right) \left(\frac{V_0 + \Delta V}{V_0}\right)^{K_{nq2}} \{1 + N_{nqf2}(\Delta f)\} \right] \tag{20}$$

Where $\Delta V = V - V_0$ and $\Delta f = f - f_0$.

Expanding using the Taylors series expansion of $(1 + x)^n = 1 + nx + \frac{n(n-1)}{2!}x^2 + \dots$ for $x \ll 1$ for the above equation and neglecting the higher terms (Δ^2) gives:

$$\Delta P_l = P - P_0 = [K_{l1} \Delta f + K_{l2} \Delta V] \tag{21}$$

$$\Delta Q_l = Q - Q_0 = [K_{l3} \Delta f + K_{l4} \Delta V] \tag{22}$$

Hence change in load ΔP_l and ΔQ_l could be expressed in terms of incremental change in voltage ΔV and incremental change in frequency Δf . The effect of decaying of oscillation could also be seen in simulation results.

Expressing the (21) & (22) in matrix form gives;

$$\begin{bmatrix} \Delta P \\ \Delta Q \end{bmatrix} = \underbrace{\begin{bmatrix} K_{l1} & K_{l2} \\ K_{l3} & K_{l4} \end{bmatrix}}_A \begin{bmatrix} \Delta f \\ \Delta V \end{bmatrix} \tag{23}$$

The Eigen value of A matrix can be found out by $|SI-A|=0$.

$$A = \begin{bmatrix} -0.9 & 0.595 \\ 0.1 & -3.9 \end{bmatrix} \text{ and the Eigen value works out to be } \alpha_1 = -0.78 \text{ \& } \alpha_2 = -4.01.$$

Since the Eigen values lies in the left half of the s-plane therefore, the load have tendency of decaying. In the small system this is very important as large non decaying oscillation will result in cascaded tripping of feeders. Generally, the inductance and capacitance in the load stores energy at rated voltage and frequency. When the voltage and frequency changes the load has tendency support the system by absorbing or releasing the stored energy. The same has been established above by finding the Eigen value of the load model.

The load constants of (21) & (22) are

$$K_{l1} = P_0 P_{C1} N_{npf};$$

$$K_{l2} = \frac{P_0}{V_0} [P_{C1} K_{np1} + K_{np2} - P_{C1} K_{np2}];$$

$$K_{l3} = P_0 Q_{C1} N_{nqf1} + Q_0 N_{nqf2} - P_0 Q_{C1} N_{nqf2};$$

$$K_{l4} = \frac{1}{V_0} [P_0 Q_{C1} K_{nq1} + Q_0 K_{nq2} - P_0 Q_{C1} K_{nq2}];$$

The aggregate effective value of indices is calculated based on proportion of various types of load in respect to the total load. Equation for establishing the aggregate index is given below.

$$N_{(ag)} = \sum_{i=1}^n N(i) \frac{kW(i)}{kW(total)} \tag{24}$$

Aggregate indices of the load are given in Table II of Appendix and load constants are given in Table III of Appendix.

IV. MODEL SIMULATION

The model developed in matlab is shown in Fig.3. Two cases have been considered for simulation as given below.



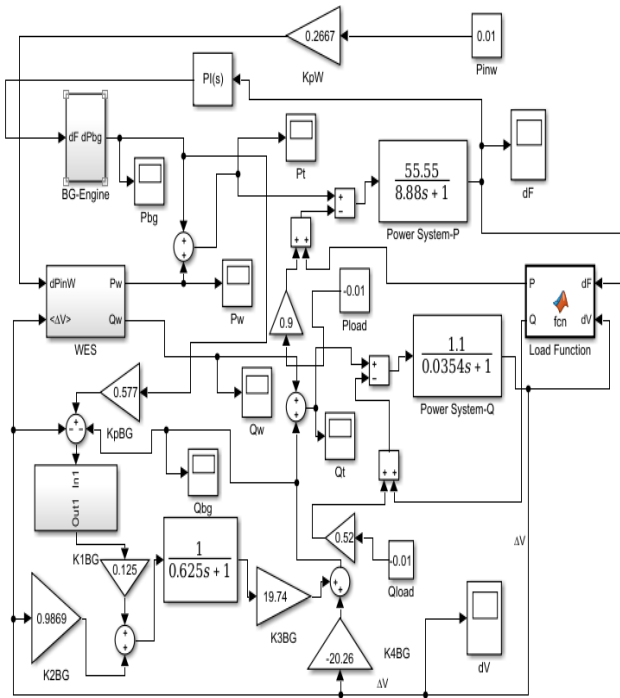
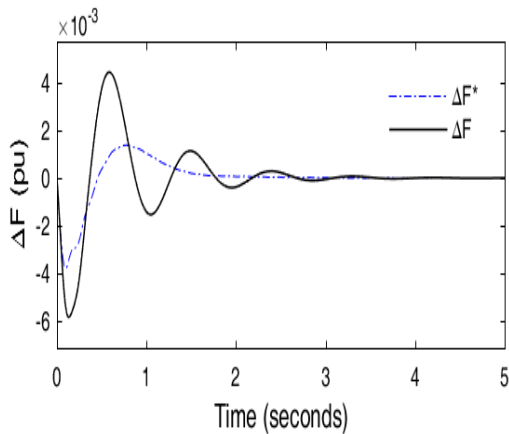


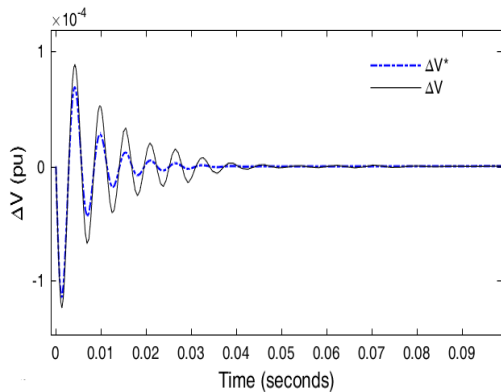
Fig.5, Transfer Function model of isolated rural microgrid consisting of Wind-BG.

A. Case-I

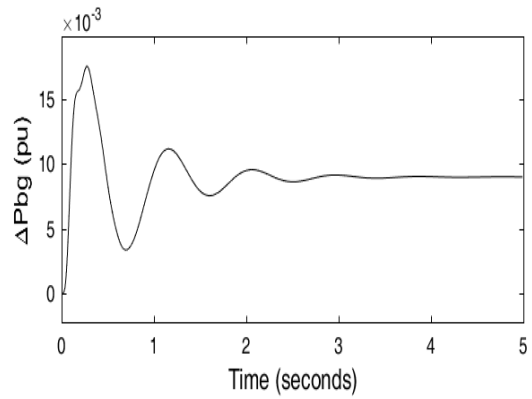
Step increase in load by 1% is considered for simulation, however, no change in input power to wind energy system. The dynamic response of the isolated microgrid for 1% increase in load (active and reactive) are shown in Fig. 6.



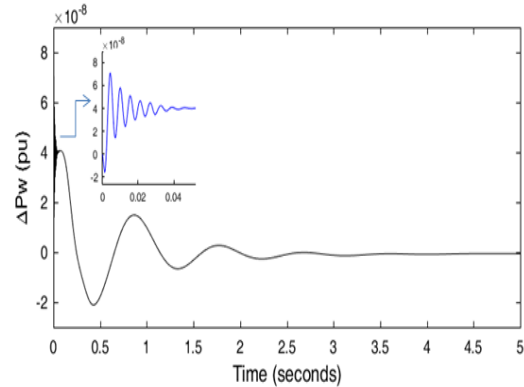
(a)



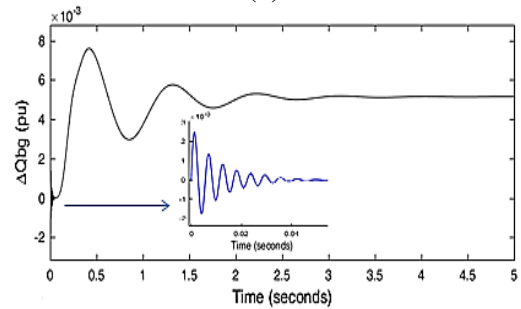
(b)



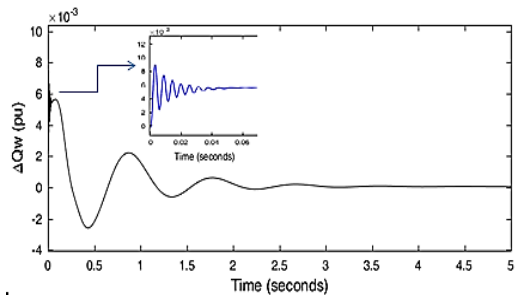
(c)



(d)



(e)

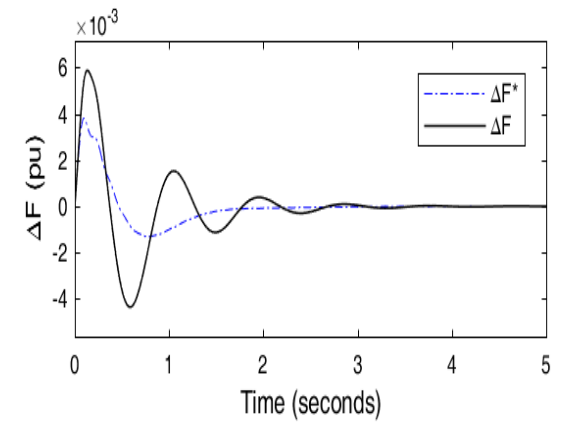


(f)

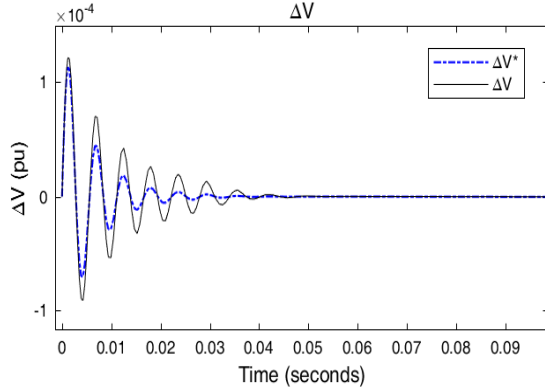
Fig.6, Dynamic response of the system for 1% step increase in load for time vs. (a)Δf (b) ΔV (c) ΔP_{bg} (d) ΔP_w (e) ΔQ_{bg} & (f) ΔQ_w.

B. Case-II

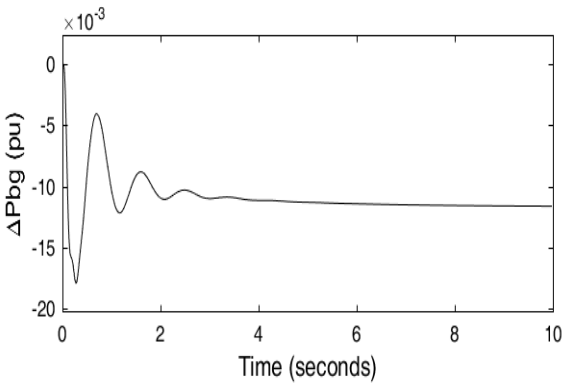
Step decrease in load by 1% has been considered along with increase in wind input power by 1%. The dynamic response of the isolated microgrid for 1% decrease in load (active and reactive) and 1% increase in wind input power are shown in Fig.7.



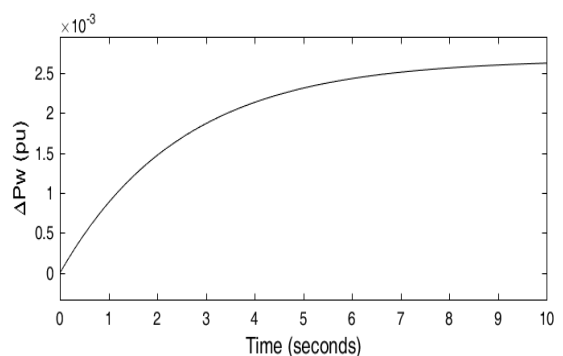
(a)



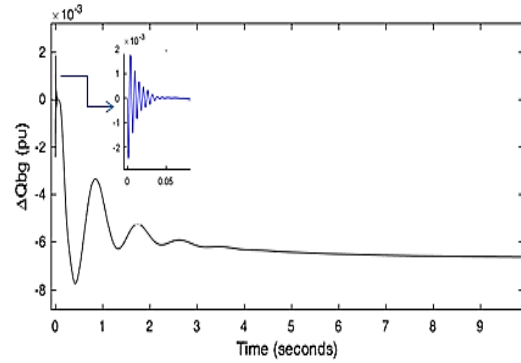
(b)



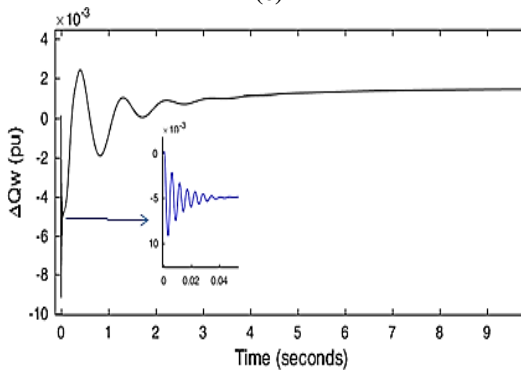
(c)



(d)



(e)



(f)

Fig.7, Dynamic response of the system for 1% step decrease in load & 1% increase in wind input power for time vs. (a)Δf (b) ΔV (c) ΔP_{bg} (d) ΔP_w (e) ΔQ_{bg} & (f) ΔQ_w.

In the first case the load increases due to which frequency and voltage decrease initially. Fig. 6(a) & (b) shows frequency and voltage oscillation including load model (ΔF & ΔV) and without inclusion of load model (ΔF^* & ΔV^*). From the frequency and voltage graph it is interpreted that frequency settles within 5s and voltage settles within 60 ms with zero steady state error. Also the effect of load on frequency and voltage could be seen. Due to inclusion of load characteristics, frequency & voltage oscillation, peak overshoot and settling time increase which cannot be interpreted only by taking the step response. Oscillations also indicates that load has tendency to captivate and release energy to the system. Further, active and reactive power requirement is taken up by BG with no change in active and reactive power being drawn from WES, refer Fig. 6(c), 6(d), 6(e) & 6(f). The active and reactive power of BG and WES reaches steady state within 5s. The time taken is due to interaction of inertia associated with BG and WES. Also from the graph it can be seen that initially reactive power is provided by the converter associated with WES and later taken up by the excitation system of BG. As per the modeling same has been verified by the dynamic response under steady state condition.

In case-II there is sudden decrease in the wind input by 1% and load decreases by 1% resulting in frequency and voltage increase initially. The graphs in Fig.7 show various parameters of the system.

The frequency settles within 5s and voltage with 60ms. Due to increase in input wind power as well as decrease in load, the active and reactive power output from BG decreases to balance the system power requirement. From Fig. 7 (c) & 7 (d) it can be seen that active power reaches steady state around 10s. This is due inertia of wind turbine. Due to which WES takes time to reach steady state. The reactive power of BG and WES, Fig 7 (e) & 7 (f) also reaches steady state within 10s. The results of the simulation are tabulated in Table VI of Appendix. Hence, the system becomes stable and achieves steady state condition.

V. CONCLUSION

Isolated rural microgrid have been modeled using EPRI load model. Aggregate incides of various types of load have been used for simulation study. Typical loads like Residential Load, Small Insdustrial Load, Adminstrartive Building & Lighting Load and Agricultrual pump load have been considered in the modeling. Also the system is modeled in such a way that any change in load requirement or increase/decrease in input power to WES is taken up by the BG system. From the study it can be interpreted that load has significant effect on dynamic stability of the system. When the system parameter changes load dynamics also changes and controllers should be tuned such that system reaches steady state with the limits within stipulated time frame. The results have been verified by taking step disturbance in load and in input power to the WES system. Frequency settles within 5s and voltage within 60ms as desired.

VI. APPENDIX

The system has been modeled considering total contract demand = 750 kW.
Max. demand with diversity factor of 0.6 = 500*0.6 = 450 kW.

MICROGRID DATA :

$$D_{ps} = \frac{\partial P_L}{\partial F} = \frac{P_L}{P_r * f_0} = 0.018 \text{ pu kW/pu Hz.}$$

$$K_{ps} = 1/D_{ps} = 55.55 \text{ pu Hz/pu kW.}$$

$$T_{ps} = \frac{2H}{f_0 D_{ps}} = 8.88 \text{ sec.}$$

$$D_{vs} = \frac{\partial Q_L}{\partial V} = \frac{Q_L}{Q_r * V} = \frac{P_L}{P_r * V} = 0.9 \text{ pu kVAR/pu kV.}$$

$$K_{vs} = 1/D_{vs} = 1.11 \text{ pu kV/pu kVAR.}$$

$$T_{vs} = 0.03538 \text{ sec. pf}=0.866, P_1=0.9\text{pu}, Q_1=0.519, f^0=50\text{Hz.}$$

Table I

Sources	Generation parameters			
	Rated Capacity (kW)	Gen (kW)	Active Power (pu)	Reactive Power (pu)
BG	250	225	0.45	0.259
Wind	250	225	0.45	0.259
Total	500	450	0.9	0.519

Table II

WES Data			
$P_w=0.45 \text{ pu kW}$		$Q_w=0.259 \text{ pu kVAR}$	
$X_{TW}=0.05 \text{ pu}$	$K_1=20.25$	$K_2=0.443$	$K_3=0.449$
$K_4=-0.449$	$K_5=19.995$	$K_6=-19.74$	$V_{inv}=1.01 \text{ pu}$
$\Delta\delta_{inv}=1.27^\circ$			

Table III

BG data			
$P_{BG}=0.45 \text{ pu}$		$Q_{BG}=0.259 \text{ pu}$	
$X_d=0.4 \text{ pu}$	$X_d'=0.05 \text{ pu}$	$T_{d0}'=5.0 \text{ sec}$	$T_B=0.625 \text{ s}$
$T_{BG1}=0.01 \text{ s}$	$T_{BG2}=0.02 \text{ s}$	$T_{BG3}=0.15 \text{ s}$	$T_{BG4}=0.2 \text{ s}$
$T_{BG5}=0.014 \text{ s}$	$T_{BG6}=0.04 \text{ s}$	$T_{BG7}=0.036 \text{ s}$	$K_{AB}=200$
$T_{AB}=0.05 \text{ s}$	$K_{EB}=1$	$T_{EB}=2.0 \text{ s}$	$K_{FB}=0.5$
$T_{FB}=1.0 \text{ s}$	$K_{1BG}=0.125$	$K_{2BG}=0.987$	$K_{3BG}=19.74$
$K_{4BG}=-20.26$			

Table IV

Load	RL	SI	LAL	PL	Aggregate Index
Indices					
N_{np1}	-2.01	0.6	-2.9	0.8	-0.9
K_{np1}	1.1	0.1	0.1	1.4	0.63
K_{np2}	0.8	0.6	0.2	1.1	0.7
N_{nq1}	-2.3	1.6	-1.8	4.2	0.63
N_{nq2}	2.8	1.9	1.2	4.8	2.62
K_{nq1}	2.6	0.6	1.6	1.4	1.43
K_{nq2}	-2.7	-1.9	-0.9	1	-1.39
Load Rating (kW)	200	300	100	150	Total 750

RL-Residential Load
SI- Small Industrial Load
LAL- Administrative Building & Lighting Load
PL- Pump Load

Table V

Load Data			
$K_{11}=-0.9$	$K_{12}=-0.595$	$K_{13}=0.1$	$K_{14}=-3.9$
$P_{C1}=0.55$	$Q_{C1}=0.7$		

Table VI

System disturbance	Case I	Case II		
	$\Delta P_1=0.009 \text{ pu}$ $\Delta Q_1=0.0052 \text{ pu}$ $\Delta P_{inw}=0$	$\Delta P_1=-0.009 \text{ pu}$ $\Delta Q_1=-0.0052 \text{ pu}$ $\Delta P_{inw}=0.00267 \text{ pu}$		
System variables	Steady state value (pu)	Settling time (sec)	Steady state value (pu)	Settling time (sec)
ΔF	0	4.5	0	4.3
ΔV	0	0.056	0	0.052
ΔP_{bg}	0.009	4.6	-0.0116	9.2
ΔP_w	0	4.8	0.0026	9.8
ΔQ_{bg}	0.0052	4.4	-0.0066	9.7
ΔQ_w	0	4.1	0.0014	9.6

REFERENCES

- Robert Lasseter, Abbas Akhil, Chris Mamay, John Stephens, "White Paper on Integration of Distributed Energy Resources, The CERTS Microgrid Concept", CERTS, April, 2002.
- N.H.S. Ray, M.K. Mohanty and R.C. Mohanty, "A Study on application of biogas as fuel in compression ignition engine", IJMET, Vol.-3, Issue-1, Oct 2013.
- M. Orabi , F. El-Sousy , H. Godah , M.Z.Youssef, "High-performance induction generator-wind turbine connected to utility grid", INTELEC 2004, 26th Annual International Telecommunications Energy Conference, IEEE.



4. Sagar P. Burud , Trishul B. Patil , Uday S. Mirje, Somesh S. More, Gauri S. Mane , Snehal S. Mulik, "Requirement of Minimum Capacitor to Build-Up and Maintain the Voltage in Self Excited Induction Generator", 2018-International Conference On Advances in Communication and Computing Technology (ICACCT), IEEE.
5. Aakriti Pandey, Ashok Kumar Pandey, "Reactive power compensation for a doubly fed induction generator based WECS", 2017 International Conference on Innovations in Information, Embedded and Communication Systems (ICIECS), IEEE.
6. P Sharma and T.S. Bhatti, "Performance Investigation of Isolated Wind-Diesel Hybrid Power Systems With WECS Having PMIG", IEEE Trans. on Industrial Electronics, Vol. 60, No. 4, April 2013.
7. Suji Muhammed, Krishnakumari V, "Performance Analysis of a PMSG Based Wind Energy Conversion System", International Journal of Engineering Research & Technology (IJERT), Vol. 3 Issue 8, August – 2014.
8. Alepuz, S., Calle, A., Busquets-Monge, S., Kouro, S., Wu, B., "Use of stored energy in PMSG rotor inertia for low-voltage ride-through in back-to-back NPC converter-based wind power systems", IEEE Trans. Ind. Electron. 2013, 60, 1787–1796.
9. Revel, G., Leon, A.E., Alonso, D.M., Muiola, J.L., Dynamics and stability analysis of a power system with a PMSG-based wind farm performing ancillary services", IEEE Trans. Circuits Syst. 2014, 61, 2182–2193.
10. D. K. Yadav, T. S. Bhatti and Ashu Verma, "Study of Integrated Rural Electrification System Using Wind-Biogas Based Hybrid System and Limited Grid Supply System", International Journal of Renewable Energy Research, Vol.7, No.1, 2017.
11. L. Wang, and Y. Lin, "Analysis of a commercial biogas generation system using a gas engine-induction generator set", IEEE Transaction on Energy Conversion, vol. 24, no.1, pp. 230-239, 2009.
12. S. R. Arya, R. Niwas, K. Kant Bhalla, B. Singh, A. Chandra and K. A. Haddad, "Power Quality Improvement in Isolated Distributed Power Generating System Using DSTATCOM," IEEE Transactions on Industry Applications, vol. 51, no. 6, pp. 4766-4774, 2015.
13. B. V. Ga and T. V. Nam, "Appropriate structural parameters of biogas SI engine converted from diesel engine," IET Renewable Power Generation, vol. 9, no. 3, pp. 255-261, 2015.
14. B. J. Seshaprasad and D. Mikkelsen, "Load Models for Power System Stability Studies", www.iitk.ac.in /npsc/papers.
15. Load representation for dynamic performance analysis [of power systems], IEEE Trans. Power Systems, Vol.8, no.2, pp. 472-482, May 1993.
16. M.Farrohabadi and K.Bhattacharya, "Frequency Control in Isolated/Islanded Microgrids through voltage regulation", IEEE Transaction, Smart Grid, Sept 2015.
17. M. Yang, S. Yuanyuan, F. Yang, S. Xiangjing, W. Chengshan , W. Jianhui, "Frequency and Voltage Coordinated Control for Isolated Wind-Diesel Power System Based on Adaptive Sliding Mode and Disturbance Observer", IEEE Transactions on Sustainable Energy, Volume: 10, Issue: 4, 2019.
18. S. Mishra, C.K. Panigraha and D.P. Kothari, "Design and simulation of a solar-wind-biogas hybrid system architecture using HOMER in India", International Journal of Ambient Energy 37(2):1-8 · December 2014.



Dr. Ashu Verma received her B.Tech degree in Electrical Engineering from NIT Hamirpur in 2001, M.Tech in Power Systems from IIT, Delhi in 2002 and PhD in Transmission Expansion Planning from Electrical Engineering Department, IIT, Delhi in 2010. She is associate professor at Centre of Energy Studies, IIT, Delhi. Her present research interest are power system planning, operation and control aspects of integrated renewable energy systems, policy and regulatory framework for enabling large scale integration of renewable energy sources in India.



Dr. T. S. Bhatti is Professor Emeritus in Centre for Energy studies. He did his PhD from IIT Delhi in 1985. He was a Post-doctoral fellow at University of Newcastle, Australia in 1987. He has published more than 150 papers in National and International Journals and Conferences. He has edited a book entitled, "Small Hydro Power Systems". He has done several Sponsored and Consultancy projects in the area of Electric Energy Systems. His current area of research includes automatic generation control of power systems, transient stability analysis of multi-machine systems, load frequency and reactive power control of isolated hybrid power systems.

AUTHORS PROFILE



Vinit Kumar Singh is a graduate in Electrical Engineering in 1999 from MNIT, Allahabad, India and Masters in Process Control Engineering in 2003 from Delhi University, India. Presently he is pursuing part time PhD (at Centre of Energy Studies) from Indian Institute of Technology, New Delhi, India. He also has 16 years of experience in Electrical Power Sector. His area of interest is Dynamic Stability study of Power System,

Microgrid and Reactive power control.